Journal of Experimental Botany, Vol. 64, No. 7, pp. 1805–1816, 2013
doi:10.1093/jxb/ert042 Advance Access publication 13 February, 2013
This paper is available online free of all access charges (see http://jxb.oxfordjournals.org/open_access.html for further details)

Journal of Experimental Botany
www.jxb.oxfordjournals.org

RESEARCH PAPER

The cytoskeleton is disrupted by the bacterial effector HrpZ, but not by the bacterial PAMP flg22, in tobacco BY-2 cells

Xin Guan[1,*], Günther Buchholz[2] and Peter Nick[1]

[1] Molecular Cell Biology, Botanical Institute, Karlsruhe Institute of Technology, Kaiserstr. 2, D-76128 Karlsruhe, Germany
[2] RLP AgroScience/AlPlanta – Institute for Plant Research, Breitenweg 71, D-67435, Neustadt an der Weinstraße, Germany

* To whom correspondence should be addressed. E-mail: xin.guan@bio.uni-karlsruhe.de

Received 16 November 2012; Revised 2 January 2013; Accepted 29 January 2013

Abstract

Plant innate immunity is composed of two layers. Basal immunity is triggered by pathogen-associated molecular patterns (PAMPs) such as the flagellin-peptide flg22 and is termed PAMP-triggered immunity (PTI). In addition, effector-triggered immunity (ETI) linked with programmed cell death and cytoskeletal reorganization can be induced by pathogen-derived factors, such as the Harpin proteins originating from phytopathogenic bacteria. To get insight into the link between cytoskeleton and PTI or ETI, this study followed the responses of actin filaments and microtubules to flg22 and HrpZ *in vivo* by spinning-disc confocal microscopy in GFP-tagged marker lines of tobacco BY-2. At a concentration that clearly impairs mitosis, flg22 can induce only subtle cytoskeletal responses. In contrast, HrpZ causes a rapid and massive bundling of actin microfilaments (completed in ~20 min, i.e. almost simultaneously with extracellular alkalinization), which is followed by progressive disintegration of actin cables and cytoplasmic microtubules, a loss of cytoplasmic structure, and vacuolar disintegration. Cytoskeletal disruption is proposed as an early event that discriminates HrpZ-triggered ETI-like defence from flg22-triggered PTI.

Key words: Actin, defence, flg22, Harpin Z, innate immunity, tobacco (*Nicotiana tabacum* L. cv. Bright Yellow 2).

Introduction

Plants lack the somatic adaptive immune system based on mobile defence cells characteristic for animal immunity. Plant defence, in contrast, is based upon an innate immunity of each individual cell (Jones and Dangl, 2006). This innate immunity comprises two distinct layers. The basal layer is evolutionarily ancient and triggered by conserved pathogen structures termed pathogen-associated molecular patterns (PAMPs). These PAMPs, such as flagellin, the subunit building the filament of bacterial flagellum, bind to specific receptors in the plasma membrane triggering so-called PAMP-triggered immunity (PTI). This basal layer of broad immunity is often accompanied by a more advanced and strain-specific immunity termed effector-triggered immunity (ETI), which is triggered by pathogen effectors that have to enter the cytoplasm of the host cell. The reason for this complexity is linked to coevolution between host and pathogen: PTI would be expected to select for pathogens, where the eliciting PAMPs are lost. However, since PAMPs are essential for the lifecycle of the pathogen, this evolutionary strategy does not work – a bacterial intruder lacking the PAMP flagellin would not elicit a PTI response, but it would also not be able to move. This dilemma stimulated, during a second round of host–pathogen warfare, the development of microbial effector proteins. These effectors are secreted into the cytoplasm of the host and suppress PTI (for review, see Tsuda and Katagiri, 2010). In response to these pathogen effectors, the host plant has evolved additional pathogen-specific receptors (encoded by so-called R genes) that specifically recognize the effectors in the cytoplasm and trigger the second layer of immunity, ETI (Boller and He, 2009). In many cases, ETI culminates in a plant-specific version of programmed cell death, the hypersensitive response,

often followed by systemic acquired resistance of the host. The conceptual dichotomy between PTI and ETI has been very valuable to interpret and classify the huge variety of plant defence responses, but this concept is presently on the move again. Recent studies show that the difference between PAMPs and effectors is more gradual than previously conceived (Thomma *et al*., 2011). Moreover, PTI and ETI share numerous common events (Tsuda and Katagiri, 2010). Thus, the apparent dichotomy might be a question of signal quantity rather than quality. In addition, plants can discriminate different pathogens and activate different responses that are appropriate for the respective pathogen. Therefore, at present, the PTI-ETI concept is extended towards a signature-based model (for review, see Aslam *et al*., 2009).

The archetypal elicitor of PTI is bacterial flagellin, which triggers defence responses in various plants (Gómez-Gómez and Boller, 2002). A synthetic 22-amino-acid peptide (flg22) from a conserved flagellin domain is sufficient to induce most of the cellular responses (Felix *et al*., 1999). A genetic screen in *Arabidopsis thaliana* using flg22 identified the *Arabidopsis* leucine-rich repeat receptor kinase FLS2, which binds flg22 (for review, see Chinchilla *et al*., 2006). Upon binding of the ligand, FLS2 is internalized by a receptor-mediated endocytic process that presumably has regulatory functions (Jones and Dangl, 2006).

To trigger ETI-like programmed cell death, Harpin proteins have been used. These bacterial proteins, first discovered in *Erwinia amylovora*, a phytopathogenic bacterium causing the fire-blight disease of apple and pears (Wei *et al*., 1992), have acquired considerable interest as triggers for hypersensitive response-like cell death and systemic acquired responses. They act as components of a bacterial type-III secretion system and can induce host events characteristic for ETI, including production of reactive oxygen species, accumulation of defence-related transcripts, and cell death (for review, see Tampakaki *et al*., 2010). Harpin proteins comprise different types that fulfil different functions during type-III secretion: HrpN is translocated into the host cytoplasm and a commercial elicitor based on HrpN was used in the current study group's previous work to mimic various aspects of ETI in grapevine suspension cells (Chang and Nick, 2012). In contrast, HrpZ, originating from the bean halo-blight pathogen, *Pseudomonas syringae* pv. *phaseolicola* ($HrpZ_{Psph}$), is localized in the apoplast and acts as helper protein supporting type-III secretion. Functional proof for a role in type-III secretion comes from experiments where HrpZ could be successfully integrated into the type III secretion model system of the mammalian pathogen *Yersinia enterocolitica* (Lee *et al*., 2001a). Furthermore, HrpZ was found to associate stably with liposomes and synthetic bilayer membranes and forms an ion-conducting pore *in vitro*. Whether HrpZ can trigger ETI of the strict sense, is not clear. The finding of pathovar-specific activities in *A. thaliana* (Haapalainen *et al*., 2012) indicates the existence of cognate R-gene products. Due to this conceptual incertainty, the term 'ETI-like' response will be used throughout the current work.

In animal cells, the host cytoskeleton is a major target of type-III effectors, in particular actin microfilaments (Cossart and Sansonetti, 2004). Although various type-III effectors of plant pathogenic bacteria can suppress plant defence responses such as hypersensitive cell death and expression of defence genes (for review, see Takemoto and Hardham, 2004), it is unclear whether they target the cytoskeleton as observed in animal cells. So far, AvrBs3, an effector from *Xanthomonas campestris*, was reported to induce swelling of mesophyll cells, a response that could be indicative of disruption to the plant microtubule, and HopZ1a, a type-III secreted effector from *P. syringae* was claimed to interact with both tubulin heterodimers and polymerized microtubules (Marois *et al*., 2002; Lee *et al*., 2012). Since several plant pathogens produce anticytoskeletal compounds during invasion (reviewed by Kobayashi and Kobayashi, 2008), the cytoskeleton seems to be an important player in plant defence. In fact, actin filaments seem to act cooperatively with PEN2 and PEN3 in penetration resistance against a broad range of pathogenic fungi (Stein *et al*., 2006). The role of the cytoskeleton has been mainly discussed in the context of barrier responses to pathogen penetration, for example, by cell-wall papillae that can be observed at sites of penetration attempts. The formation of these papillae is preceded by a reorganization of the cytoskeleton, causing redistribution of vesicle traffic and cytoplasmic aggregation towards the penetration site (for reviews, see Takemoto and Hardham, 2004; Kobayashi and Kobayashi, 2008) and a somewhat slower migration of the nucleus (for review, see Schmelzer, 2002). In addition, the cytoskeleton participates in the execution of hypersensitive cell death that involves and requires massive remodelling of actin filaments and microtubules (for review, see Smertenko and Franklin-Tong, 2011).

This study group's previous work addressed the role of the cytoskeleton in Harpin-triggered defence using two cell lines from *Vitis* that differ in their microtubular dynamics manifested by altered levels of tyrosinylated α-tubulin (Qiao *et al*., 2010). The line *Vitis vinifera* cv. Pinot Noir is susceptible to pathogens such as *Plasmopara viticola* and *Erysiphe necator*, whereas *Vitis rupestris* efficiently copes with infection by these pathogens (Jürges *et al*., 2009). Treatment with a commercial HrpN preparation could trigger various defence responses, including extracellular alkalinization and induction of defence genes. However, these defence responses were weaker and less sensitive in the cell line, where microtubules were more dynamic. In response to the elicitor, the cortical microtubules disappeared, which was most pronounced in *V. rupestris*. This correlation indicated that stable microtubules act as negative regulators of defence signalling and are disrupted in response to the elicitor. If this is more than a correlation, pharmacological manipulation of microtubules should be able to activate defence genes. In fact, using resveratrol synthase and stilbene synthase as key genes of phytoalexin induction, it could be shown that pharmacological manipulation of microtubules could induce gene expression in the absence of Harpin (Qiao *et al*., 2010), suggesting that the cytoskeleton might play a third role in plant defence. In addition to its function in barrier responses to penetration attempts, and in the execution of hypersensitive cell death, it might also act more upstream in defence signalling. Using the

same cellular system, early defence responses were compared to flg22 (PTI, not leading to cell-death) and Harpin (ETI-like response, culminating in cell death) and it was shown that both responses shared some of early signal components, but differed in perception, the signature of oxidative burst, and the integration into a qualitatively different stilbene output, correlated with different cell-death responses (Chang and Nick, 2012).

Both flg22 and Harpin affected cortical microtubules and actin filaments, which was more pronounced in the *V. rupestris* line and for treatment with Harpin. However, since the cytoskeleton had to be visualized by either immunofluorescence (microtubules) or by fluorescent phalloidin (actin filaments), both requiring fixation of the cells, only the bulk changes of the cytoskeleton occurring at progressive stages of the response became detectable. To get clearer insight into the timing of the response, the current work investigated the tobacco BY-2 system. In this system, GFP-tagged marker lines for the cytoskeleton have been established, which allows the following the cytoskeletal response over time in living cells and thus also detection of the earlier stages of cytoskeletal remodelling. The cellular responses of BY-2 to flg22 (PTI) and HrpZ (ETI-like response) are compared with focus on the cytoskeleton. Consistent with the results from grapevine cells, strong and rapid cytoskeletal responses to HrpZ were observed, contrasting with very mild changes triggered by flg22. However, extending previous results by spinning-disc confocal microscopy and life-cell imaging, it is now shown that these responses initiate early and proceed in parallel with extracellular alkalinization (so far, one of the most rapid readouts for defence). This shows that cytoskeletal remodeling might channel early signaling between HrpZ-triggered ETI-like defence and flg22-triggered PTI.

Materials and methods

Cell lines and cultivation

BY-2 (*Nicotiana tabacum* L. cv. Bright Yellow-2) suspension cell lines (Nagata *et al*., 1992) were cultivated in liquid medium containing 4.3 g l^{-1} Murashige and Skoog salts (Duchefa Biochemie; containing l^{-1}: 30 g sucrose, 200 mg KH_2PO_4, 100 mg *myo*-inositol, 1 mg thiamine, and 0.2 mg 2,4-dichlorophenoxyacetic acid, final pH 5.8). In addition to the non-transformed BY-2 wild type, transgenic lines were used in this study that expressed the actin-binding domain 2 of plant fimbrin in fusion with GFP under control of the constitutive CaMV 35S promoter (AtFABD2, Sano *et al*., 2005) and a transgenic line expressing the β-tubulin AtTuB6 from *A. thaliana* in fusion with GFP driven by the CaMV 35S promoter (Hohenberger *et al*., 2011). The cells were subcultivated weekly by inoculating 1.0–1.5 ml stationary cells into 30 ml fresh medium in 100 ml Erlenmeyer flasks. The cells were incubated in darkness at 27 °C under constant shaking on a KS260 basic orbital shaker (IKA Labortechnik) at 150 rpm. The media for the transgenic cell lines were complemented with either 30 mg l^{-1} hygromycin (GFP-AtFABD2) or with 50 mg l^{-1} kanamycin (GFP-AtTuB6), respectively.

Elicitors

The flg22 peptide QRLSTGSRINSAKDDAAGLQIA (Felix *et al*., 1999) was purchased from a commercial source (Laboratoire de Biotechnologie du Luxembourg). The gene for the expression of HrpZ from *P. syringae* p.v. *phaseolicola* ($HrpZ_{Pph}$) was cloned into the vector pET21a (Novagen, Darmstadt, Germany) and transferred into *Escherichia coli* BL21 (DE3) RIL (Agilent Technologies, USA) by electroporation (Li *et al*. 2005). The recombinant protein was expressed and purified as follows. The transformed cells were grown at 30 °C in LB with 100 mg l^{-1} ampicillin to an optical density at 600 nm approximately 0.6–0.8. Then, expression was induced with 1 mM isopropyl β-D-1-thiogalactopyranoside for about 6 h at 30 °C. Cells were spun down and the sediment resuspended in extraction buffer (50 mM Tris-HCl pH 8.0, 100 mM NaCl, 1 mM EDTA, 1 mM phenylmethanesulphonyl fluoride, freshly added). Cells were lysed by sonication and proteins denatured by boiling for 10 min. Cell debris and denatured proteins were removed by centrifugation (4 °C, 21,000 *g*, 10 min) and the supernatant transferred to a fresh beaker. Then, solid ammonium sulphate was slowly added to 45% (w/v) of a saturated solution while stirring the mixture on ice. The precipitated protein was resuspended in 5 mM MES (pH 5.5) and desalted by dialysis using regenerated cellulose tubular membrane (size exclusion 6 kDa, wall thickness 30 μM; ZelluTrans/Roth dialysis membranes T2, Roth, Karlsruhe, Germany). The concentration of purified HrpZ was quantified by the amido black protein dye assay (Popov *et al*., 1975) against bovine serum albumin as calibration reference.

Microscopy

The response of actin filaments (using the GFP-AtFABD2 marker) and microtubules (using the GFP-AtTuB6 marker) to flg22 or HrpZ was followed over time in individual cells by spinning-disc confocal microscopy. Confocal images were recorded with an AxioObserver Z1 (Zeiss, Jena, Germany) using a 63 × LCI-Neofluar Imm Corr DIC objective (NA 1.3), the 488 nm emission line of an Ar-Kr laser, and a spinning-disc device (YOKOGAWA CSU-X1 5000). The cells on the slide were maintained at 27 °C by in microscope temperature control stage and time-lapse series recorded by capturing Z-stack every 2 min over a period of 20 min (for flg22), or every 20 min over a period of 120 min (for HrpZ). The responses were elicited by 10 μM (flg22) or 57.6 μM (HrpZ). The long-term response was assessed from Z-stack collected from single recordings at lower concentrations at 3 day (for flg22, 100 nM) and 2 day (for HrpZ, 2.59 μM) after treatment. Mock controls were done with the respective solvents (water for flg22 and 5 mM MES for HrpZ) and treated in exactly the same manner as the samples.

Measurement of extracellular alkalinization

Extracellular alkalinization was measured by combining a pH meter (pH 12, Schott Handylab) with a pH electrode (LoT 403-M8-S7/120, Mettler Toledo). BY-2 cells were pre-equilibrated on an orbital shaker for around 30 min and then treated with different concentrations of flg22 (1–500 nM) or HrpZ (0.26–14.4 μM). Values for ΔpH were calculated as differentials of treatment versus mock control. Peak values were used as estimate for ΔpH_{max} and were reached at around 600 s (10 min) for flg22 and around 900–1200 s (15–20 min) for HrpZ. As positive controls for the activity of HrpZ, suspension cell lines from *V. rupestris* and *V. vinifera* cv. Pinot Noir (Qiao *et al*., 2010; Chang and Nick, 2012) were added to the study.

Phenotyping of cellular responses

Packed cell volume as indicator for growth was determined at day 3 after subcultivation/treatment. Aliquots (2 ml) were sampled from the culture flask with a sterile, scaled pipette (Greiner) while shaking to ensure a homogenous distribution of cells, the pipettes sealed with Nescofilm and positioned vertically at 4 °C till full sedimentation of the cells. The packed cell volume was determined from the scale of the pipettes. Mitotic index was determined in aliquots of 500 μl at day 3 after subcultivation/treatment after staining for 2 min with 10 ng ml^{-1}

Hoechst 33258 (Sigma-Aldrich, Neu-Ulm, Germany) and addition of one drop of 10% (v/v) Triton X-100 (Roth). Cells were immediately scored under a AxioImager Z.1 using a DAPI filter set (excitation at 365 nm, beam splitter at 395 nm, and emission at 445 nm) by means of a Fuchs-Rosenthal haematocytometer (Thoma, Freiburg, Germany). For each data point, 2000 cells obtained from three independent experimental series were scored. To monitor changes in cell shape, differential interference contrast images of central sections were acquired by the AxioImager Z.1 in the ApoTome mode at day 3 after subcultivation/treatment using the mosaic and length measurement tools of the AxioVision software. As measure of cell shape, the ratio of cell width over cell length was measured and clustered into 11 classes increasing in steps of 0.2 and one class with values >2.0. Frequency distributions were constructed for three independent experimental series of 300–500 individual cells measured for each repeat. Mortality was assessed according to the method by Gaff and Okong'O-Ogola (1971) using 2.5% (w/v) Evans Blue (Sigma-Aldrich) in aliquots of 200 µl using custom-made staining chambers to remove the medium. The frequency of the dead cells (stained in blue) was scored using a Fuchs-Rosenthal haematocytometer under bright-field illumination with a AxioImager Z.1/ApoTome microscope. Mortality values were determined from three independent experiments with 1500 cells scored for each data point. To evaluate division synchrony (Campanoni *et al*., 2003), frequency distributions over the number of cells per individual file were constructed from approximately 2000 cell files from three independent experimental series.

Results

Actin responses to flg22 are subtle; those to HrpZ are drastic

To gain insight into the earlier stages of cytoskeleton remodelling in plant defence, this study followed the response of actin filaments to flg22 and HrpZ in individual BY-2 cells expressing the GFP-AtFABD2 marker by spinning-disc confocal microscopy. To ensure saturation of possible responses even for early time points, 10 µM flg22 was used, based on dose–response studies (to be discussed). Z-stack were collected through the entire cell every 2 min after addition of flg22 through the first 20 min (Fig. 1A). The transvacuolar network of actin cables emanating from the nucleus did not reveal any significant changes (Fig. 1A, upper row). However, a response of the fine meshwork of the cortical actin filaments underneath the cell membrane became detectable from ~5–10 min after elicitation (Fig. 1A, middle and lower rows). Here, the finer filaments disappeared and cortical actin cables changed orientation and often became more prominent (for instance, compare the images for 20 min

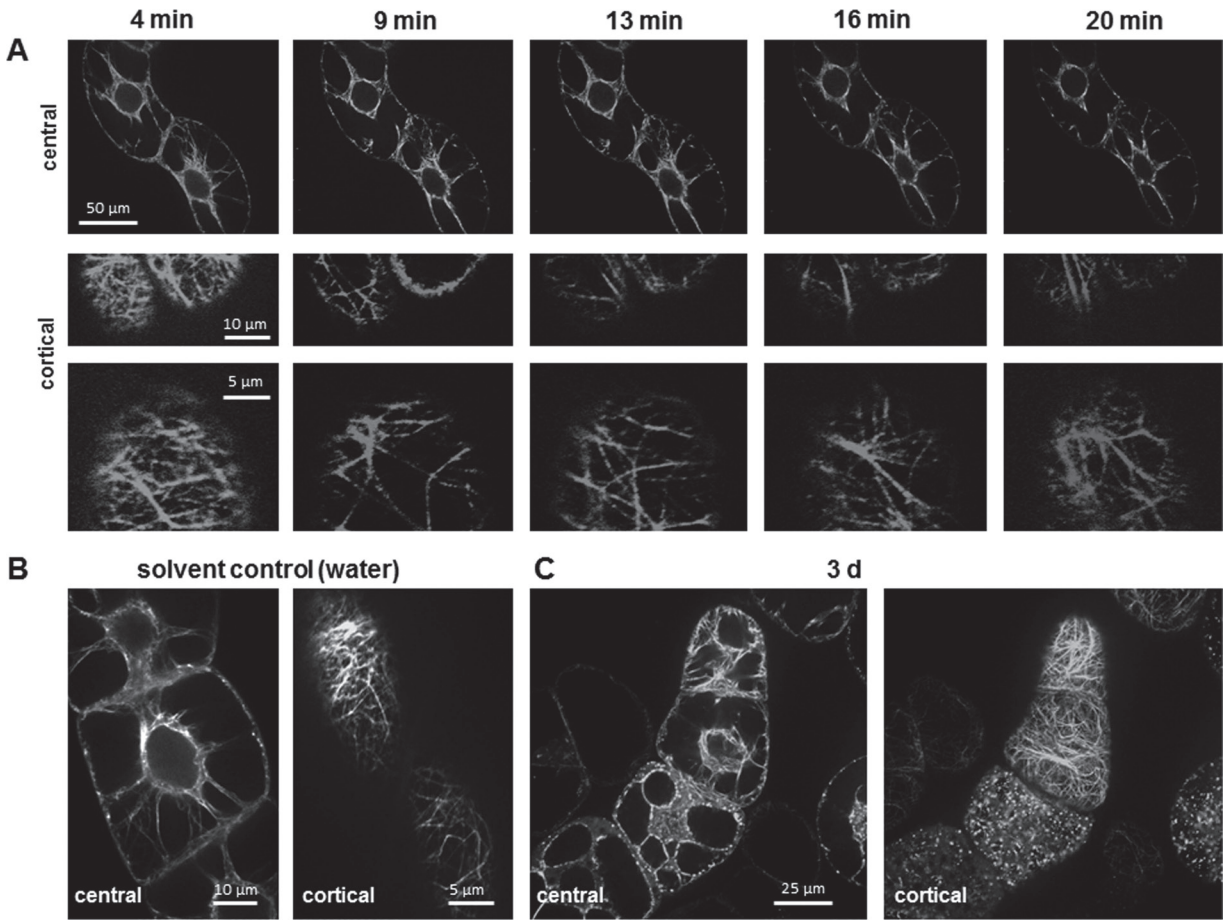

Fig. 1. Response of actin filaments in BY-2 to flg22 *in vivo* visualized by the GFP-AtFABD2 marker and spinning-disc confocal microscopy. (A) Time series after treatment with 10 µM flg22; upper row, merged Z-stack of confocal sections showing the layers in cell centre; middle and lower rows, details from two cortical regions of the same cell. (B) Solvent control (water). (C) Long-term response (3 days) after elicitation with 100 nM flg22. Observations are representative of at least five independent experimental series with a population of 100 individual cells for each treatment. Bars, 50, 10, and 5 µm (A), 10 and 5 µm (B), and 25 µm (C).

versus 4 min in the middle row of Fig. 1A). A responsiveness of the cortical actin meshwork was also observed in long-term studies using lower concentrations of flg22 such as 100 nM (Fig. 1C), where actin filaments in many (but not all) cells disintegrated into punctuate arrays, whereas the perinuclear network still persisted. None of these responses was observed in the mock control (Fig. 1B).

The rather subtle actin response to flg22 was in contrast to the drastic changes induced by HrpZ (Fig. 2). Merged Z-stack of confocal sections showing the layers in cell centre (upper row) and the cortical regions of the same cell (middle row) demonstrated that actin filaments had already undergone disruption at 20 min after elicitation with 57.6 μM HrpZ. Differential-interference contrast images of these cells showed that this disruption was accompanied by a dramatic breakdown of cytoplasmic architecture manifest at 60 min after elicitation and a disintegration of the vacuole (white arrows) visible at 90 min after elicitation. This was not observed in the solvent control (5 mM MES buffer). An inspection of earlier time points showed that actin filaments condensed into cortical aggregations that were clearly detectable at 10 min after elicitation (Supplementary Fig. S1A, available at *JXB* online) followed by contraction of actin towards the nucleus. A long-term experiment conducted at a ~20-fold reduced concentration (2.59 μM HrpZ), where most cells survived, as deduced from mortality scores (to be discussed), produced cortical actin filaments that were bundled and disorganized (Supplementary Fig. S1B).

Microtubules respond to HrpZ, but not to flg22

Parallel to actin, this study followed the response of microtubules using the GFP-AtTuB6 marker (Fig. 3). In the vast majority of cells, a treatment with 10 μM flg22 did not cause any changes, neither in the radial microtubules emanating from the nucleus (Fig. 3A, upper row) nor in the cortical microtubules underneath the membrane (Fig. 3A, lower row). Even for a long-term treatment, these microtubules did not respond (data not shown). However, in rare cases, aberrant microtubule structures could be observed (Supplementary Fig. S2). In these cells, plaque-like agglomerations of signals appeared in the vicinity of the nuclear envelope either as a transient stage in response to a high concentration of flg22 (10 μM), or as long-term response to lower concentration (100 nM). As already found for actin, treatment with HrpZ (57.6 μM) caused drastic changes, mainly in the radial microtubules which were found to be eliminated (Fig. 3B, upper row), whereas cortical microtubules became thinner as compared to the control, but still maintained their integrity (Fig. 3B, lower row).

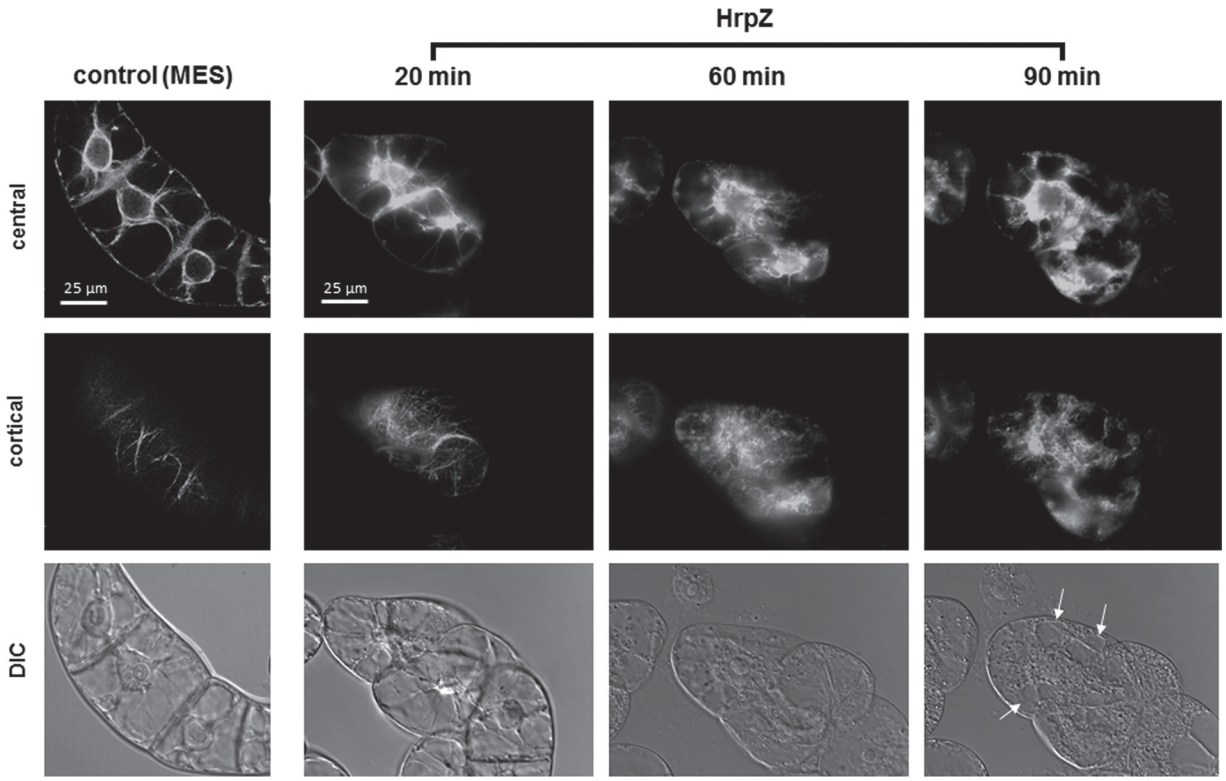

Fig. 2. Response of actin filaments in BY-2 to HrpZ *in vivo* visualized by the GFP-AtFABD2 marker and spinning-disc confocal microscopy; time series after treatment with a saturating concentration of HrpZ (57.6 μM); upper row, merged Z-stack of confocal sections showing the layers in cell centre; middle and lower rows, confocal sections and differential-interference contrast (DIC) images of cortical regions of the same cell, showing the breakdown of cytoplasmic architecture manifest at 60 min after elicitation and the disintegration of the vacuole (white arrows) at 90 min after elicitation. The solvent control consisted in 5 mM MES buffer. Observations are representative of at least five independent experimental series with a population of 100 individual cells for each treatment. Bars, 25 μm.

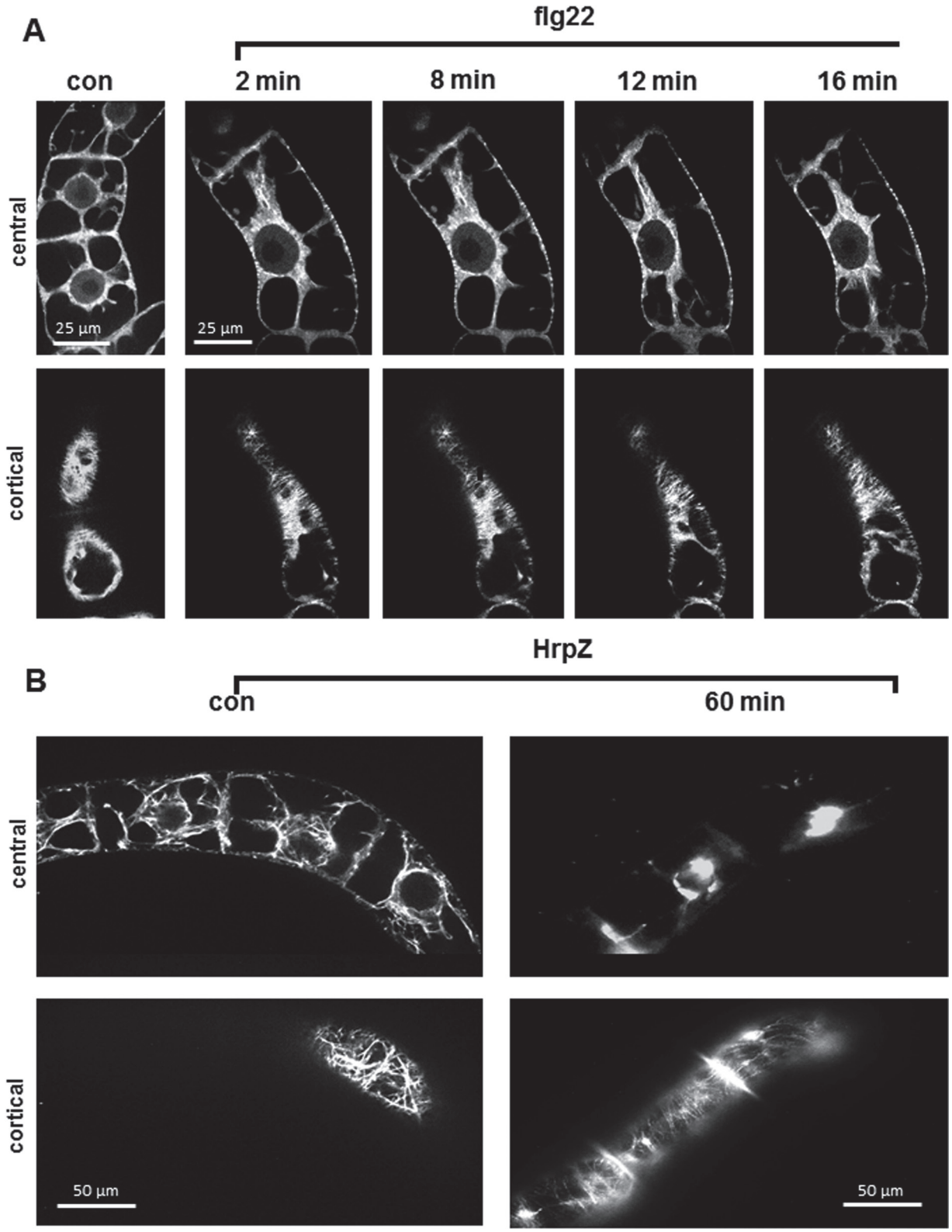

Fig. 3. Response of microtubules in BY-2 to 10 µM flg22 (A) or 57.6 µM HrpZ (B) *in vivo* visualized by the GFP-AtTuB6 marker and spinning-disc confocal microscopy, showing merged Z-stack of confocal sections showing the layers in cell centre and the cortical regions of the same cell. Controls (con) show the response to the solvent (A water, B 5 mM MES buffer). Observations are representative of at least five independent experimental series with a population of 100 individual cells for each treatment. Bars, 25 µm (A) and Bars, 50 µm (B).

Apoplastic alkalinization as rapid defence readout is more sensitive to flg22 than HrpZ

One of the earliest responses detected is a modification of plasma membrane permeability, in particular Ca^{2+}, H^+, and K^+ and anion fluxes that can be conveniently followed as changes of extracellular pH (Jabs *et al.*, 1997; reviewed in Felix *et al.*, 1999; Nürnberger and Scheel, 2001). To test, whether the differential cytoskeletal response to flg22 versus HrpZ was caused by a lack of sensitivity of BY-2 cells to flg22, this study therefore used extracellular alkalinization as a fast cellular response monitoring plant defence. Already at a low concentrations (1 nM), flg22 could trigger a pH reaching a maximum at ~600 s after elicitation (Fig. 4A). This peak increased in amplitude, but was not advanced in time, when the concentration of flg22 was increased. A dose–response of maximal alkalinization over the concentration of flg22 showed a saturation of the response from 200 nM at 0.27 pH units (Fig. 4B). HrpZ in a concentration of 1.73 µM could trigger an alkalinization that was comparable in amplitude (Fig. 4C). To verify that this recombinantly produced elicitor was biologically active, the same concentration of HrpZ was tested in the two grapevine cell lines. For the more responsive *V. rupestris*, up to almost 0.7 pH units were obtained, for the less responsive *V. vinifera* cv. Pinot Noir the response was close to that found in BY-2. This pattern shows that the activity of HrpZ used in the current experiments was comparable to that of the commercial Harpin elicitor used in the previous studies (Qiao *et al.*, 2010; Chang and Nick, 2012). A dose–response of maximal alkalinization over the concentration of HrpZ in BY-2 (Supplementary Fig. S3) showed that stronger alkalinization can be induced in BY-2 as well, but that this requires higher concentrations of the elicitor as compared to *V. rupestris* indicating differences in sensitivity between these cell lines. It should also be mentioned that the time points when these maxima were reached were between 900 and 1500 s, depending on the concentration, which is significantly later than the timing found for flg22 (Fig. 4A).

Cell division and cellular morphogenesis are altered by HrpZ

The morphogenesis of plant cells depends on the cytoskeleton. The cytoskeletal responses induced by HrpZ should therefore, as a consequence, alter cellular morphogenesis. Therefore, this study phenotyped growth, cell shape, and division synchrony as sensitive targets of cytoskeletal remodelling. A dose–response curve of packed cell volume as reporter for culture growth over the concentration of elicitor (Fig. 5A) showed a significant inhibition with increasing concentration of flg22 or HrpZ, respectively. This inhibition became more prominent with time (compare the curves for days 3 and 4 in Fig. 5A). To test, whether the decreased growth was caused by inhibition of cell division, the dose–responses of mitotic index were monitored at day 3 (at the peak of mitotic activity) after inoculation. For flg22, even for a high concentration of 1 µM flg22, mitotic index was only partially reduced (by some third as compared to the control). In contrast,

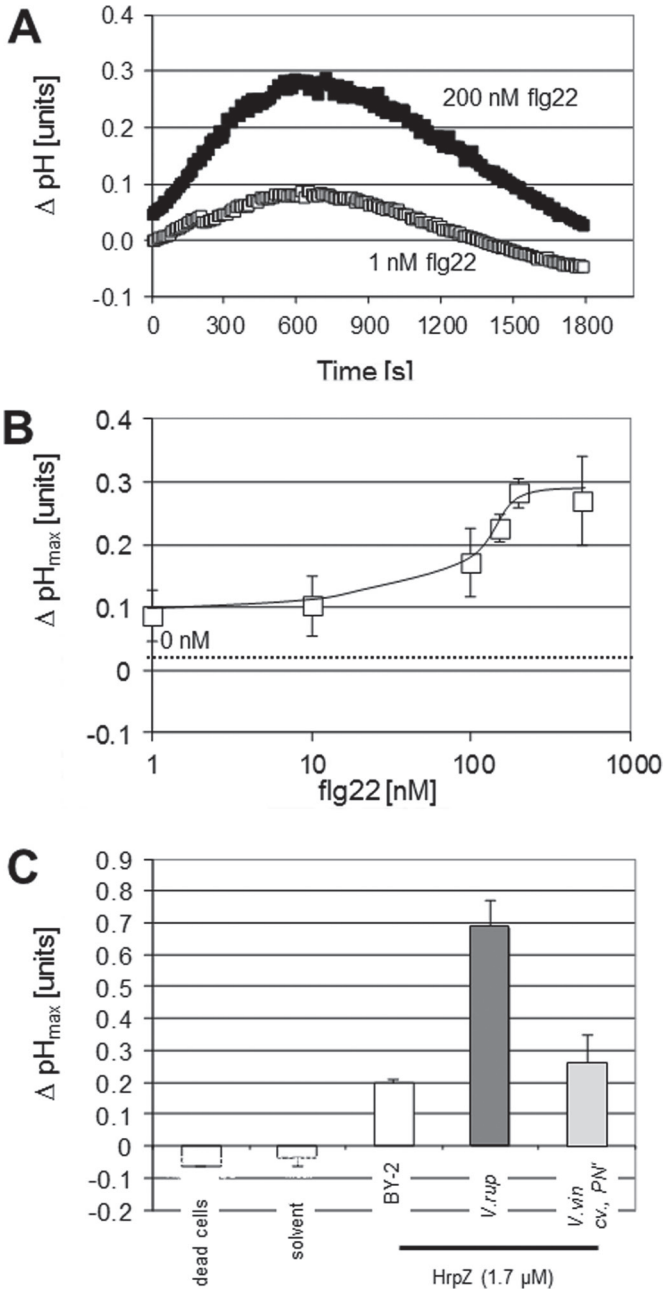

Fig. 4. Extracellular alkalinization in response to flg22 (A and B) or HrpZ (C). (A) Representative time course of BY-2 cells to a low (1 nM) and a high (200 nM) concentration of flg22. (B) Dose-response of maximal alkalinization over the concentration of flg22 in BY-2; dotted line shows the value obtained for solvent control water. (C) Maximal alkalinization for treatment with 1.73 µM HrpZ in BY-2 (white bars), the highly responsive *V. rupestris* cell line (dark grey), and the weakly responsive *V. vinifera* cv. 'Pinot Noir' cell line (light grey); negative controls include dead BY-2 cells challenged by the elicitor and a solvent control (5 mM MES); the response of the cells is recorded at the respective maxima (520 s after induction for BY-2, 1600 s after induction for the two *Vitis* cell lines). Data in (B) and (C) are mean ± standard errors from three independent biological replicates.

HrpZ reduced the mitotic index drastically to almost zero (Fig. 5B). The effects of flg22 and HrpZ on cell shape were investigated, since the axiality of cell expansion depends on the organization of cortical microtubules, Frequency distributions for the ratio between cell width over cell length were constructed (Fig. 5C). For high concentrations of flg22 such as 1 μM, the frequency of cells with ratios of width/length 0.4–0.6 decreased, whereas cells with ratios >1 increased. This means that elongated cells became rare; whereas broader cells became more frequent (Fig. 5D left). This trend became progressively evident from flg22 concentrations exceeding 10 nM. The situation was inverse for treatments with HrpZ. Here the frequency of cells with a ratio of width/length 0.2–0.4 increased for as the elicitor concentration reached 1.73 μM, which means that cells became progressively elongated (Fig. 5D right). Lower concentrations of HrpZ were not effective in affecting cell shape (data not shown).

Since the effects of flg22 on cellular morphogenesis were very subtle in comparison with those of HrpZ, division synchrony was used as the most sensitive morphological marker. Cell divisions in tobacco suspension cells are synchronized by signals that depend on polar auxin transport which can be monitored as frequency peak of cells composed of six cells (Campanoni *et al*., 2003). Since polar auxin transport is strongly dependent on actin organization (reviewed in Nick, 2010), the division synchrony can be used as highly sensitive marker for actin remodelling and had been used successfully to monitor cell-death-related actin bundling (Chang *et al*., 2011). In response to flg22, the amplitude of this peak increased progressively up to 3-fold as compared to the control (Supplementary Fig. S4), suggesting that flg22 can modulate the actin cytoskeleton although this is not accompanied by bulk changes. Conversely, as to be expected from its actin bundling effect, a permissive concentration of HrpZ (2.59 μM) elevates the frequency of hexacellular files (Supplementary Fig. S4).

HrpZ, but not flg22, can induce cell death

A characteristic feature of ETI is programmed cell death, leading to a hypersensitive response occurring at infection sites. Therefore, this study followed mortality in response to flg22 and HrpZ over time. For flg22, elevated mortality was not observed for a range of concentrations (Fig. 6 left). Even for treatment with 200 nM (data not shown), mortality was only 3.4% at day 3. On the contrary, HrpZ induced cell death from day 2, reaching nearly 70% at day 3 after treatment with 8.64 μM HrpZ (Fig. 6 right).

Discussion

This work addressed the response of the cytoskeleton to flg22 (a canonical trigger for PTI) and HrpZ (a bacterial elicitor triggering an ETI-like response) by spinning-disc confocal microscopy and life-cell imaging in the BY-2 tobacco cell line. The motivation was the observation that a commercial Harpin elicitor induced cytoskeletal responses in two grapevine cell lines that differ in their microtubular dynamics (Qiao *et al*., 2010). A limitation of the grapevine system was the need to visualize microtubules by immunofluorescence, and actin by fluorescent phalloidin, both protocols requiring chemical fixation. Since the cytoskeletal response could thus not be followed over time in individual cells, only bulk changes of cytoskeletal organization became evident, which means that the early stages of these responses were not detected. This limitation was circumvented in the current work by using tobacco BY-2 cells, where transgenic fluorescent marker lines are available. A second drawback of the previous experimental system was the fact that the commercial Harpin elicitor is a HrpN species, which requires translocation into the host cytoplasm. Therefore, this study used HrpZ, which acts as helper protein supporting for type-III secretion in the apoplastic face of the membrane. Based on these two changes, it is now shown that the cytoskeletal responses differ depending on the nature of the elicitor and the nature of the cytoskeletal element: whereas both actin and microtubules responded drastically and rapidly to HrpZ, the cytoskeletal responses to flg22 remained very subtle. Both responses initiated early and could be detected from ~5–10 min after elicitation. The time course for the actin response either accompanied (for flg22) or even preceded (for HrpZ) extracellular alkalinization, a very early response for defence, preceding calcium influx, mitogen activated protein (MAP) kinases, reactive oxygen species and plant hormones (salicylic acid, jasmonate, ethylene), and induction of defence-related genes. Generally, actin responded more sensitively as compared to microtubules, although the microtubules in the cell centre disintegrated in response to HrpZ (parallel with actin filaments).

To understand the differential early cytoskeletal response to flg22 versus HrpZ, it is relevant to compare the perceptive mechanisms for these elicitors. The PAMP flg22 is a ligand of the leucine-rich repeat receptor kinase FLS2 (Gómez-Gómez and Boller, 2000; Zipfel *et al*., 2004; Chinchilla *et al*., 2006). A dose–response curve using apoplastic alkalinization as readout shows that around 100 nM were required to elicit a significant response (Fig. 4B), which places BY-2 into the less responsive systems. For comparison, cell lines of *V. rupestris* produce a half-maximal response at <5 nM flg22, whereas, on the other hand, *V. vinifera* cv. Pinot Noir needs >800 nM flg22 for half-activation (Chang and Nick, 2012). Although BY-2 does not classify for being highly flg22 sensitive, flg22 is clearly sensed at much lower concentrations as compared to HrpZ, where >5 μM are required to get half-maximal alkalinization (Supplementary Fig. S3), consistent with findings in grapevine cells (Chang and Nick, 2012). Both elicitors also differ in the timing of apoplastic alkalinization, HrpZ occurs about 5–10 min later as compared to flg22 leading to a model, where the link between flg22 and alkalinization is more direct, whereas the link between Harpin and alkalinization is indirect. Again, this difference in timing is not confined to BY-2, but has also been observed in the grapevine system (Chang and Nick, 2012).

The low sensitivity to HrpZ indicates that this elicitor is not perceived through a canonical protein receptor, consistent with findings from other groups: For $HrpZ_{Psph}$ from

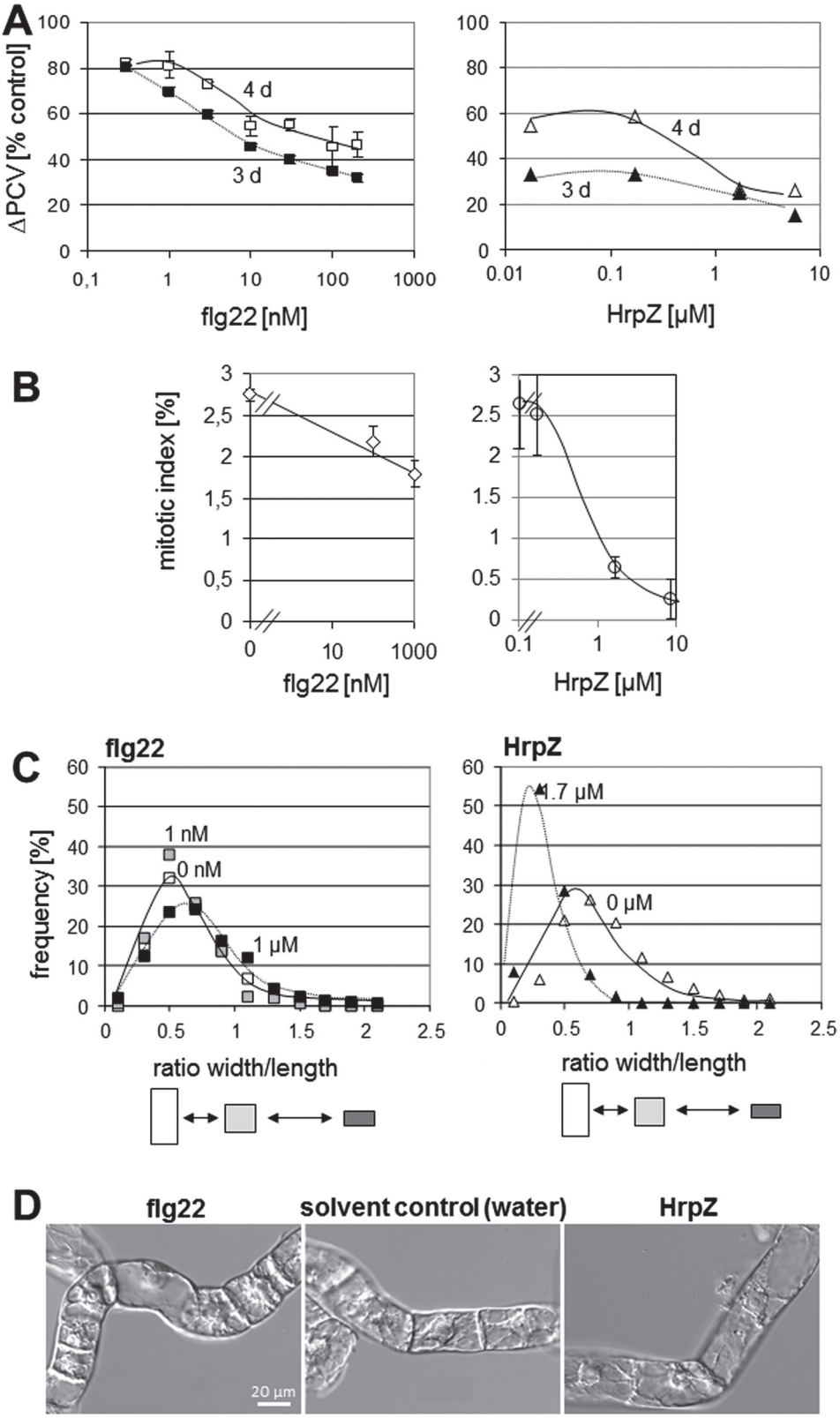

Fig. 5. Cellular responses to flg22 (left) and HrpZ (right). (A) Dose–response of packed cell volume as indicator of culture growth at day 3 (peak of mitotic activity) and day 4 (onset of cell expansion) after inoculation, respectively. (B) Dose-response of mitotic index at day 3 after inoculation (scored from a population of 2000 individual cells for each data point). (C) Effect on cell shape; frequency distributions for the ratio between cell width over cell length were constructed from 2500 individual cells for each experiment. (D) Differential-interference contrast images of representative cells either raised under control conditions (centre) or after treatment with either 1 μM flg22 or 1.73 μM HrpZ. Data in (A) and (B) are mean ± standard errors from three biological replicates.

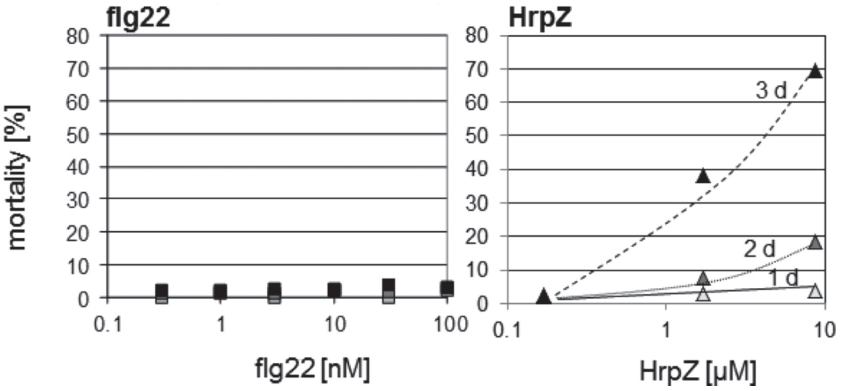

Fig. 6. Mortality in response to flg22 (left) and HrpZ (right). Data are mean ±standard errors from three independent experimental series with a population of 2000 individual cells scored after staining with 2.5% Evans Blue.

P. syringae, cation-permeable pores have been reported (Lee *et al*., 2001a). HrpZ is highly conserved in *P. syringae* strains and, unlike the harpin HrpN of *E. amylovora* which is an essential pathogenicity factor (Wei *et al*. 1992), seems to act as helper protein supporting type-III secretion. Instead of being translocated into the host cytoplasm, HrpZ has been localized in the apoplast (Brown *et al*., 2001). HrpZ can bind to phosphatidic acid and, upon insertion into vesicles prepared from plant plasma membranes, it can cause vesicle disruption (Lee *et al*., 2001b; Haapalainen *et al*., 2011). Despite this obviously different mode of perception for HrpZ, there seems to be some sort of specificity: when HrpZ proteins originating from two different pathovars of *P. syringae* were administered to *A. thaliana*, both HrpZ types caused cell death but the modulation of anionic currents was specific, and in a phage display screen for peptide binding, different motif preferences were observed (Haapalainen *et al*., 2012).

Thus, whereas the flg22 signal is transduced by a classical receptor kinase activity, the HrpZ signal acts by a localized loss of membrane integrity, which will directly impinge upon cortical actin. Actin is known to stabilize membrane integrity in a great number of systems (Papakonstanti *et al*., 2000; for review, see Koivusalo *et al*., 2009) and seems to be directly linked with the plasma membrane of plant cells as demonstrated by TIRF-microscopy in BY-2 protoplasts expressing the GFP-FABD2 marker (Hohenberger *et al*., 2011). This membrane-associated actin population on the one hand stabilizes membrane integrity (Hohenberger *et al*., 2011) and sensitively responds to perturbations of membrane integrity by rapid detachment from the plasma membrane, which is then followed by bundling of actin cables, contraction towards the nucleus, and programmed cell death (Berghöfer *et al*., 2009). The current observations integrate well into the accumulating body of evidence linking actin remodelling with programmed cell death across eukaryotic cells in general (for review, see Gourlay and Ayscough, 2005; Franklin-Tong and Gourlay, 2008) and plant cells in particular (Smertenko and Franklin-Tong, 2011). For instance, during self-incompatibility in poppy, actin remodelling is necessary and sufficient to activate programmed cell death in the male gametophyte (Thomas *et al*., 2006). Conversely, the programmed cell death of embryonic suspensors during the somatic embryogenesis of conifers requires actin remodelling which is necessary for the embryo proper to become committed for embryogenesis (Smertenko *et al*., 2003).

The link between impaired membrane integrity by HrpZ-induced pore formation and actin remodelling will be the topic of future investigations. A molecular candidate for this link might be reactive oxygen species, since they not only participate in the signalling culminating in programmed cell death (for review, see Gechev *et al*., 2006), but also trigger actin reorganization in plant programmed cell death (Wilkins *et al*., 2011). The remodelling of actin in response to changes of redox potential is observed across all eukaryotic kingdoms pointing to ancient origins (Franklin-Tong and Gourlay, 2008). In fact, when in Harpin-triggered grapevine cells the NADPH oxidase as major source of apoplastic oxidative burst was blocked by diphenylene iodonium chloride, or when apoplastic hydrogen peroxide was scavenged by addition of catalase, this impaired the induction of stilbene synthase, a key player for grapevine phytoalexin synthesis (Chang *et al*., 2011).

Compared to actin, the response of microtubules seems to be more indirect. Even at the time when the actin cytoskeleton is breaking down in response to HrpZ, cortical microtubules, although disturbed in their orientation, still maintain a certain degree of integrity (Fig. 3B). Since plant microtubules have been recently shown to respond to oxidative imbalance (Livanos *et al*., 2012), they might simply respond to the actin-dependent oxidative burst caused by pore formation. Microtubules modulate deformation-sensitive calcium channels (Ding and Pickard, 1993; Mazars *et al*., 1997) and therefore modulate apoplastic alkalinization (Chang and Nick, 2012). Alkalinization in response to Harpin elicitors occurs later as compared to that triggered by flg22 in both BY-2 (this work) and grapevine (Chang and Nick, 2012). This might be caused by the time span required for the reactive oxygen species to disassemble the microtubules modulating the calcium channel. Oryzalin and taxol could activate defence genes in the absence of Harpin elicitors in grapevine, indicating a function of microtubules upstream of gene induction (Qiao *et al*., 2010). Interestingly, latrunculin B and

phalloidin were less effective, consistent with a more indirect mode of interaction.

This study arrives at a model where a dynamic population of cortical actin acts as a sensor for membrane damage. In response to the membrane pores produced by HrpZ, actin is bundled followed by a contraction of actin cables towards the nucleus, whereas on the other hand, a rapid oxidative burst is generated (Chang and Nick, 2012) that is followed by cell death. In contrast, flg22 produces only a subtle cytoskeletal response, which might be related to the slower and weaker oxidative burst induced by flg22 as compared to Harpin elicitors (Chang and Nick, 2012). Apoplastic alkalinization as early readout of defence, however, seems to be more closely linked with flg22 as compared to Harpin elicitors. Thus, although both elicitors are generating an oxidative burst and an apoplastic alkalinization, the temporal signature differs. The response of submembraneous actin might be responsible for the generation of this temporal signature. Future work will be directed to understanding the role of the cortical cytoskeleton in decoding the temporal signature of defence activating different outputs (cell death versus basal immunity).

Supplementary material

Supplementary data are available at *JXB* online.

Supplementary Fig. S1. Early response of actin filaments in BY-2 to HrpZ and bundling of cortical actin filaments in BY-2.

Supplementary Fig. S2. Aberrant microtubule structures in response to flg22.

Supplementary Fig. S3. Dose-response of maximal alkalinization over the concentration of HrpZ in BY-2.

Supplementary Fig. S4. Division synchrony at the end of cell division phase.

Acknowledgements

This work was supported by the BACCHUS Interreg project and a fellowship of the Chinese Scholarship Council to Xin Guan. We would like to thank Dr Yubin Kashef (Zoology Institute Cell and Developmental Biology, Karlsruhe Institute of Technology, Karlsruhe), for training and support in spinning-disc confocal microscopy, and Sabine Purper for technical support with the cell lines. Use of the laboratory at RLP AgroScience/AlPlanta (Neustadt an der Weinstraße, Germany) is gratefully acknowledged.

References

Aslam SN, Erbs G, Morrissey KL, Newman MA, Chinchilla D, Boller T, Molinaro A, Jachson RW, Cooper RM. 2009. Microbe-associated molecular pattern (MAMP) signatures, synergy, size and charge: influences on perception or mobility and host defence responses. *Molecular Plant Pathology* **10,** 375–387.

Berghöfer T, Eing C, Flickinger B, Hohenberger P, Wegner LH, Frey W, Nick P. 2009. Nanosecond electric pulses trigger actin responses in plant cells. *Biochemical and Biophysical Research Communications* **387,** 590–595.

Boller T, He SY. 2009. Innate immunity in plants: an arms race between pattern recognition receptors in plants and effectors in microbial pathogens. *Science* **324,** 742–744.

Brown IR, Mansfield JW, Taira S, Roine E, Romantschuk M. 2001. Immunocytochemical localization of HrpA and HrpZ supports a role for the transfer of effector proteins from *Pseudomonas syringae* pv. *tomato* across the host plant cell wall. *Molecular Plant–Microbe Interactions* **14,** 394–404.

Campanoni P, Blasius B, Nick P. 2003. Auxin transport synchronizes the pattern of cell division in a tobacco cell line. *Plant Physiology* **133,** 1251–1260.

Chang X, Heene E, Qiao F, Nick P. 2011. The phytoalexin resveratrol regulates the initiation of hypersensitive cell death in *Vitis*. *PLoS ONE* **6,** e26405.

Chang X, Nick P. 2012. Defence signalling triggered by Flg22 and Harpin is integrated into a different stilbene output in *Vitis* cells. *PLoS ONE* **7,** e40446.

Chinchilla D, Bauer Z, Regenass M, Boller T, Felix G. 2006. The *Arabidopsis* receptor kinase FLS2 binds flg22 and determines the specificity of flagellin perception. *The Plant Cell* **18,** 465–476.

Cossart P, Sansonetti PJ. 2004. Bacterial invasion: the paradigms of enteroinvasive pathogens. *Science* **304,** 242–248.

Ding JP, Pickard BG. 1993. Mechanosensory calcium-selective cation channels in epidermal cells. *The Plant Journal* **3,** 83–110.

Felix G, Duran J D, Volko S, Boller T. 1999. Plants have a sensitive perception system for the most conserved domain of bacterial flagellin. *The Plant Journal* **18,** 265–276.

Franklin-Tong VE, Gourlay CW. 2008. A role for actin in regulating apoptosis/programmed cell death: evidence spanning yeast, plants and animals. *The Biochemical Journal* **413,** 389–404.

Gaff DF, Okong'O-Ogola O. 1971. The use of non-permeating pigments for testing the survival of cells. *Journal of Experimental Botany* **22,** 756–758.

Gechev TS, Van Breusegem F, Stone JM, Denev I, Laloi C. 2006. Reactive oxygen species as signals that modulate plant stress responses and programmed cell death. *Bioessays* **28,** 1091–1101.

Gómez-Gómez L, Boller T. 2000. FLS2: an LRR receptor-like kinase involved in the perception of the bacterial elicitor flagellin in *Arabidopsis*. *Molecular Cell* **5,** 1003–1011.

Gourlay CW, Ayscough KR. 2005. The actin cytoskeleton: a key regulator of apoptosis and ageing? *Nature Reviews Molecular Cell Biology* **6,** 583–589.

Haapalainen M, Dauphin A, Li CM, Bailly G, Tran D, Briand J, Bouteau F, Taira S. 2012. HrpZ harpins from different *Pseudomonas syringae* pathovars differ in molecular interactions and in induction of anion channel responses in *Arabidopsis thaliana* suspension cells. *Plant Physiology and Biochemistry* **51,** 168–174.

Haapalainen M, Engelhardt S, Küfner I, Li CM, Nürnberger T, Lee J, Romantschuk M, Taira S. 2011. Functional mapping of harpin HrpZ of *Pseudomonas syringae* reveals the sites responsible for protein oligomerization, lipid interactions and plant defence induction. *Molecular Plant Pathology* **12,** 151–166.

Hohenberger P, Eing C, Straessner R, Durst S, Frey W, Nick P. 2011. Plant actin controls membrane permeability. *Biochimica et Biophysica Acta* **1808,** 2304–2312.

Jabs T, Tschöpe M, Colling C, Hahlbrock K, Scheel D. 1997. Elicitor stimulated ion fluxes and O_2^- from the oxidative burst are essential components in triggering defense gene activation and phytoalexin synthesis in parsley. *Proceedings of the National Academy of Sciences, USA* **94,** 4800–4805.

Jones JD, Dangl JL. 2006. The plant immune system. *Nature* **444,** 323–329.

Jürges G, Kassemeyer HH, Dürrenberger M, Düggelin M, Nick P. 2009. The mode of interaction between *Vitis* and *Plasmopara viticola* Berk. & Curt. Ex de Bary depends on the host species. *Plant Biology* **11,** 886–898.

Kobayashi I, Kobayashi Y. 2008. Microtubules and pathogen defence. *Plant Cell Monographs* **143,** 121–140.

Koivusalo M, Kappus A, Grinstein S. 2009. Sensors, transducers, and effectors that regulate cell size and shape. *Journal of Biological Chemistry* **284,** 6595–6599.

Lee AHY, Hurley B, Felsensteiner C, *et al.* 2012. A bacterial acetyltransferase destroys plant microtubule networks and blocks secretion. *PLoS Pathogens* **8,** e100252.

Lee J, Klüsener B, Tsiamis G, *et al.* 2001a. $HrpZ_{Psph}$ from the plant pathogen *Pseudomonas syringae* pv. *phaseolicola* binds to lipid bilayers and forms an ion-conducting pore *in vitro*. *Proceedings of the National Academy of Sciences, USA* **98,** 289–294.

Lee J, Klessig DF, Nürnberger T. 2001b. A harpin binding site in tobacco plasma membranes mediates activation of the pathogenesis-related gene HIN1 independent of extracellular calcium but dependent on mitogen-activated protein kinase activity, *The Plant Cell* **13,** 1079–1093.

Li CM, Haapalainen M, Lee J, Nürnberger T, Romantschuk M, Taira S. 2005. Harpin of *Pseudomonas szringae* pv. *phaseolicola* harbors a protein binding site. *Molecular Plant–Microbe Interactions* **18,** 60–66.

Livanos P, Galatis B, Quader H, Apostolakos P. 2012. Disturbance of reactive oxygen species homeostasis induces atypical tubulin polymer formation and affects mitosis in root-tip cells of *Triticum turgidum* and *Arabidopsis thaliana*. *Cytoskeleton* **69,** 1–21.

Marois E, Van den Ackerveken G, Bonas U. 2002. The *Xanthomonas* type III effector protein AvrBs3 modulates plant gene expression and induces cell hypertrophy in the susceptible host. *Molecular Plant–Microbe Interactions* **15,** 637–646.

Mazars C, Thion L, Thuleau P, Graziana A, Knight MR, Moreau M, Ranjeva R. 1997. Organization of cytoskeleton controls the changes in cytosolic calcium of cold-shocked *Nicotiana plumbaginifolia* protoplasts. *Cell Calcium* **22,** 413–420.

Nagata T, Nemoto Y, Hasezawa S. 1992. Tobacco BY-2 cell line as the 'HeLa' cell in the cell biology of higher plants. *International Review of Cytology* **132,** 1–30.

Nick P. 2010. Probing the actin-auxin oscillator. *Plant Signaling and Behavior* **5,** 4–9.

Nürnberger T, Scheel D. 2001. Signal transmission in the plant immune response. *Trends in Plant Science* **6,** 372–379.

Papakonstanti EA, Vardaki EA, Stournaras C. 2000. Actin cytoskeleton: a signaling sensor in cell volume regulation. *Cell Physiology and Biochemistry* **10,** 257–264.

Popov N, Schmitt S, Matthies H. 1975. Eine störungsfreie Mikromethode zur Bestimmung des Proteingehaltes in Gewebehomogenaten. *Acta Biologia et Medica Germica* **34,** 1441–1446.

Qiao F, Chang X, Nick P. 2010. The cytoskeleton enhances gene expression in the response to the Harpin elicitor in grapevine. *Journal of Experimental Botany* **61,** 4021–4031.

Sano T, Higaki T, Oda Y, Hayashi T, Hasezawa S. 2005. Appearance of actin microfilament 'twin peaks' in mitosis and their function in cell plate formation, as visualized in tobacco BY-2 cells expressing GFP-fimbrin. *The Plant Journal* **44,** 595–605.

Schmelzer E. 2002. Cell polarization, a crucial process in fungal defence. *Trends in Plant Science* **7,** 411–415.

Smertenko A, Franklin-Tong VE. 2011. Organisation and regulation of the cytoskeleton in plant programmed cell death. *Cell Death and Differentiation* **18,** 1263–1270.

Smertenko AP, Bozhkov PV, Filonova LH, von Arnold S, Hussey PJ. 2003. Re-organisation of the cytoskeleton during developmental programmed cell death in *Picea abies* embryos. *The Plant Journal* **33,** 813–824.

Stein M, Dittgen J, Sánchez-Rodríguez C, Hou BH, Molina A, Schulze-Lefert P, Lipka V, Somerville S. 2006. *Arabidopsis* PEN3/PDR8, an ATP binding cassette transporter, contributes to nonhost resistance to inappropriate pathogens that enter by direct penetration. *The Plant Cell* **18,** 731–746.

Takemoto D, Hardham AR. 2004. The cytoskeleton as a regulator and target of biotic interactions in plants. *Plant Physiology* **136,** 3864–3876.

Tampakaki AP, Skandalis N, Gazi AD, Bastaki MN, Sarris PF, Charova SN, Kokkinidis M, Panopoulos NJ. 2010. Playing the 'Harp': evolution of our understanding of hrp/hrc genes. *Annuual Review of Phytopathology* **48,** 347–370.

Thomas SG, Huang S, Li S, Staiger CJ, Franklin-Tong VE. 2006. Actin depolymerization is sufficient to induce programmed cell death in self-incompatible pollen. *Journal of Cell Biology* **174,** 221–22.

Thomma BP, Nürnberger T, Joosten MH. 2011. Of PAMPs and effectors: the blurred PTI-ETI dichotomy. *The Plant Cell* **23,** 4–15.

Tsuda K, Katagiri F. 2010. Comparing signalling mechanisms engaged in pattern-triggered and effector-triggered immunity. *Current Opinion in Plant Biology* **13,** 459–465.

Wei ZM, Laby RJ, Zumoff CH, Bauer DW, He SY, Collmer A, Beer SV. 1992. Harpin, elicitor of the hypersensitive response produced by the plant pathogen *Erwinia amylovora*. *Science* **257,** 85–88.

Wilkins KA, Bancroft J, Bosch M, Ings J, Smirnoff N, Franklin-Tong VE. 2011. ROS and NO mediate actin reorganization and programmed cell death in the self-incompatibility response of *Papaver*. *Plant Physiology* **156,** 404–416.

Zipfel C, Robatzek S, Navarro L, Oakeley EJ, Jones JD, Felix G, Boller T. 2004. Bacterial disease resistance in *Arabidopsis* through flagellin perception. *Nature* **428,** 764–767.